Available online at www.sciencedirect.com
SCIENCE DIRECT®
Icarus 180 (2006) 8–22
ICARUS
www.elsevier.com/locate/icarus

Modelling meteor ablation in the venusian atmosphere

Jonathan P. McAuliffe *, Apostolos A. Christou

Armagh Observatory, College Hill, Armagh BT61 9DG, UK

Received 14 January 2005; revised 4 July 2005

Available online 12 September 2005

Abstract

A comparative study of meteor ablation in the atmospheres of the Earth and Venus is presented. The classical single body meteor ablation model is extended to incorporate a heat penetration depth estimate allowing the simulation of larger meteoroids, than would an isothermal model. The ablation of icy and rocky meteoroids, with densities of 1.0 and 3.4 g cm^{-3}, respectively, and initial radii of up to ∼8 mm for rock and ∼13 mm for ice (equivalent to an initial mass of 10^{-2} kg in both cases), was simulated in both atmospheres. In general venusian meteors are brighter than terrestrial equivalents. Large, slow, rocky objects may be up to 0.7 mag brighter on Venus, while small, icy particles with entry speeds in the range 30–60 km s^{-1}, are found to be upwards of 2.7 mag brighter than at the Earth. Venusian meteors reach maximum brightness at greater altitudes than would similar particles at the Earth. Rocky meteoroids have their points of maximum brightness some 15–35 km higher up at Venus, between 90 and 120 km, whereas, for icy particles this altitude difference is about 5–25 km higher up than at the Earth, in the range 100–125 km. These findings agree, for the most part, with recent analytical studies. Venusian meteors, which last from 100 ms to ∼1.5 s, tend to be shorter-lived than terrestrial meteors, with correspondingly shorter visible trails. Large (∼10^{-2} kg), slow (∼10 km s^{-1}) icy particles reach a maximum magnitude of ∼ −2 at Venus and remain visible for about one second, with a large section of the smaller faster meteoroids simulated here remaining visible for several hundred milliseconds. In light of recent space-based meteor observations at the Earth [Jenniskens, P., Tedesco, E., Muthry, J., Laux, C.O., Price, S., 2002. Meteorit. Planet. Sci. 37, 1071–1078], such brightness, height and duration estimates as suggested in this work, may be used in developing future observational campaigns to be carried out from Venus orbit.

Keywords: Meteors; Meteoroids; Venus; Atmosphere

1. Introduction

When the orbital path of a meteoroid intersects that of a planet with a thick atmosphere the meteoroid may, depending on its size, velocity and composition, produce a meteor upon entry. The study of meteors plays an important role in our understanding of the minor body population of the Solar System and currently, meteor data comprises the largest database of orbital information on Solar System objects. The IAU Meteor Data Center in Lund, Sweden has orbital data on almost 70,000 objects (Lindblad, 2001) and the AMOR project in New Zealand has a database containing ∼10^6 orbits (Baggaley et al., 2001). Also, observational campaigns such as the European Fireball Network continually add to this total, detecting (in the case of the EFN) large meteors at a rate of ∼50 per year (Oberst et al., 1998).

Most research in the field of meteor physics to-date, and all observational studies, have concentrated on meteor phenomena in the atmosphere of the Earth (Bronshten, 1983; Ceplecha et al., 1998; Campbell-Brown and Koschny, 2004). However, since the early 1980s a number of theoretical works have looked at meteor phenomena in extra-terrestrial atmospheres. Moses (1992) looked at how meteor ablation in the atmosphere of Neptune affects its chemical composition, while Ip (1990) examined ablation processes in the nitrogen-rich atmosphere of Saturn's moon Titan. In the case of Jupiter, Grebowsky (1981) and Kim et al. (2001)

* Corresponding author. Fax: +44 28 3752 7174.
E-mail address: jma@star.arm.ac.uk (J.P. McAuliffe).

0019-1035/$ – see front matter
doi:10.1016/j.icarus.2005.07.012

studied meteoric deposition and ionisation effects, and a host of authors have investigated meteor phenomena and their effects in the martian atmosphere (Shafrir, 1967; Flynn and McKay, 1990; Davis, 1993; Adolfsson et al., 1996; Pesnell and Grebowsky, 2000). As for venusian meteors, Apshtein et al. (1982) looked at how meteor observations at Venus (and Mars) might be used to glean information on the atmosphere's structure, while Beech (1998) and Christou (2004) investigated the possibility of detectable venusian meteor shower activity.

The study of meteors in the atmospheres of other planets will allow the extension of our understanding of meteor phenomena, to include information about the meteoroid population outside a narrow torus centered on the Earth's orbit. It will increase the size of the sample of meteoroid streams available for study, and indirectly the number of known comet or asteroid parent bodies. Off-Earth observational campaigns would allow current meteor ablation models to be tested under entirely different circumstances than can be done using only the terrestrial meteor population. Through the study of meteors or meteor showers associated with the same parent body but at different planets (e.g., 1P/Halley meteors at the Earth, Mars, and Venus; Christou, 2004), we could examine the ablation of the components of a meteoroid stream under different atmospheric conditions and obtain a greater understanding of the association between meteors and their parent bodies. Although not examined in this work, understanding meteor ablation in Venus' atmosphere given its similarity to the early terrestrial atmosphere, might allow estimates to be made of the entry survivability potential of organic material, which may have seeded the primordial Earth with the precursors of life (Jenniskens, 2001; Coulson, 2002).

This paper looks at the ablation of venusian meteors. We numerically model the mass-loss, deceleration and luminescence of meteoroids in Venus' atmosphere. In Section 2 we develop a single-body pseudo-thermal ablation model based on that of Moses (1992). In Section 3 we discuss the results of applying this model to meteoroids in the 10^{-8}–10^{-2} kg range, entering the venusian atmosphere with initial speeds of 10–80 km/s and entry angles of 45°. We model two types of meteoroid—chondritic stone and water ice, the thermal parameters for which are taken from Podolak et al. (1988). Finally, we look at how our results compare to analytical predictions and what these results mean in terms of possible in situ observational studies.

2. Method

The single-body meteor ablation model requires the solution of a set of coupled ordinary differential equations, each describing the variation of a specific meteor parameter with time or, as may be more intuitive, with decreasing height. Here we develop the model used by Moses (1992) to incorporate a pseudo-thermal heat–depth estimate mechanism (see Section 2.2.1). This technique allows us to model larger objects than would the standard isothermal single-body ablation model.

2.1. Atmospheric flow regime

When a meteoroid enters a planet's atmosphere it is bombarded by atmospheric molecules which deliver energy and momentum to the incoming particle, heating it and slowing it down. At heights at which most ablation takes place the mean free path of the atmosphere λ_{mfp}, is on the order of several tens of centimeters, for example, in the case of the Earth, λ_{mfp} varies from 12 cm at 100 km to 83 cm at 110 km. Campbell-Brown and Koschny (2004) used a simple collisional model, to study the ability of the meteoric vapour cloud produced during ablation, to prevent atmospheric particles from directly impacting the meteoroid surface. They found that for sub-millimeter meteoroids at 96 km, where λ_{mfp} is about 6 cm, only around one in every million atmospheric particles is prevented from reaching the meteoroid by the vapour cloud. Implicitly then, at greater altitudes where the atmospheric mean free path is larger, this shielding effect would be further reduced allowing even bigger particles to ablate under free-flow conditions. In this work we therefore assume that for meteoroids with initial sizes on the order of a centimeter that ablation takes place under such conditions of free molecular flow. For larger objects, ablating at lower altitudes, this assumption breaks down however, as the ablating meteoroid passes through a transition zone and into a continuum flow regime (Ceplecha et al., 2000). In this study we limit ourselves to the use of a free molecular flow model.

2.2. Ablation equations

2.2.1. Energy balance equation

The energy or heat balance between an atmosphere and a meteoroid was first tackled by Whipple (1950, 1951) in his studies of micrometeoroid interaction with the Earth's atmosphere. In the case of a spherical, homogeneous, rapidly rotating meteoroid the standard energy balance equation takes the form

$$\frac{\Lambda}{2}\pi r^2 \rho_{\mathrm{a}} v^3 + \pi r^2 S(1-\alpha) = \frac{4}{3}\pi r^3 \rho_{\mathrm{m}} c \frac{\mathrm{d}T_{\mathrm{m}}}{\mathrm{d}t} + 4\pi r^2 \epsilon_{\mathrm{rad}} \sigma \left(T_{\mathrm{m}}^4 - T_{\mathrm{a}}^4\right) - L\frac{\mathrm{d}m}{\mathrm{d}t}. \quad (1)$$

The terms on the left-hand side constitute energy input, the first being the energy the meteoroid obtains during collisions with atmospheric constituents. The second term specifies the energy gain due to solar radiation at a particular planet's heliocentric distance. The contribution of this term is negligible for all but the earliest stages of entry. The accommodation coefficient Λ, sometimes referred to as the heat-transfer coefficient, represents the fraction of the kinetic energy of the atmospheric molecules transferred to the

meteoroid during collisions and subsequently used in heating and ablation. For the limiting case where the thermal speed of the atmospheric molecules $v_{\rm th}$, is much less than the meteoroid's speed v, the accommodation coefficient is calculated using the following expression (Hood and Horanyi, 1991)

$$\Lambda = 1 - \frac{1}{2s_{\rm a}^2}\left(\frac{\gamma+1}{\gamma-1}\right)\frac{T_{\rm m}}{T_{\rm a}}, \tag{2}$$

where $s_{\rm a} = v/v_{\rm th}$, and γ is the ratio of the specific heat of the terrestrial atmospheric gases at constant pressure to that at constant volume ($\sim$7/5)—a similar value will be assumed for the γ of the venusian atmospheric gases. For the lifetime of all meteors modelled in this study the value of Λ remains close to unity. The other symbols constituting the terms on the left-hand side of Eq. (1) are the meteoroid radius r, the atmospheric density $\rho_{\rm a}$, the solar constant S, and α the meteoroid material's albedo. The energy consumption terms on the right-hand side include, as ordered, a meteoroid heating term, a radiative cooling term and an evaporative mass loss term (see Section 2.2.2). The quantities that make up these terms are the meteoroid bulk density $\rho_{\rm m}$, its specific heat capacity c, the meteoroid temperature $T_{\rm m}$, the thermal emissivity $\epsilon_{\rm rad}$, the Stefan–Boltzmann constant σ, the atmospheric temperature $T_{\rm a}$, and the latent heat of vaporisation L. Values for these and other parameters used in the model are found in Table 1. As is clear, Eq. (1) varies with time, but using the following time–height relationship

$$\frac{{\rm d}h}{{\rm d}t} = -v\cos\theta, \tag{3}$$

where θ is the angle a meteoroid's velocity vector makes with the normal to the atmosphere at interface, we can determine the atmospheric height of the meteoroid at any stage of the meteor's flight. Reformulating Eq. (1) we express the rate of meteoroid heating as

$$\frac{{\rm d}T_{\rm m}}{{\rm d}t} = \left(\frac{4}{3}\pi r^3\rho_{\rm m}c\right)^{-1}\left(\frac{\Lambda}{2}\pi r^2\rho_{\rm a}v^3 + \pi r^2 S(1-\alpha) - 4\pi r^2\epsilon_{\rm rad}\sigma\left(T_{\rm m}^4 - T_{\rm a}^4\right) + L\frac{{\rm d}m}{{\rm d}t}\right). \tag{4}$$

Note the use of $T_{\rm m}$ in the above equations. This quantity denotes the isothermal temperature of a meteoroid heated uniformly throughout and therefore requires the assumption that no thermal gradients exist within the body. Such an assumption imposes an upper limit on the size of particles to which the model may be applied since for larger objects heat conduction and temperature gradients become important. Love and Brownlee (1991) (hereafter L&B91) used an expression for a material's Biot number (Bi) given by Eq. (5), to determine an upper limit of isothermality of $\sim$1 mm, above which differential heating within the body is assumed to become important;

$$Bi = hl/K. \tag{5}$$

Table 1
Meteoroid properties

Property	Units	Rock	Water ice
α, albedo[a]	%	3.0	3.0
c, specific heat[a]	J kg^{-1} K^{-1}	9.6×10^2	4.2×10^3
δ, density[a]	kg m^{-3}	3.4×10^3	1.0×10^3
ϵ, emissivity[c]	%	1.0	1.0
$T_{\rm melt}$[a]	K	1800	273
L, latent heat < $T_{\rm melt}$[a]	J kg^{-1}	8.1×10^6	2.8×10^6
L, latent heat > $T_{\rm melt}$[a]	J kg^{-1}	6.7×10^6	2.5×10^6
μ, mass unit[c]	kg	8.3×10^{-26}	3.0×10^{-26}
K, thermal conductivity[d]	W m^{-1} K^{-1}	2.0	1.6
A (Eq. (9))[b]	Dimensionless	13.176	11.5901
B (Eq. (9))[b]	K	24605.0	2104.2

[a] Values taken from Moses (1992).
[b] Values taken from Podolak et al. (1988).
[c] Unity assumption for emissivity, see Hunten et al. (1980).
[d] Values taken from Adolfsson et al. (1996).

Here, h is *a* heat transfer coefficient, however it is not *the* heat transfer coefficient denoted previously by Λ. In this work it will be used in determining the depth of heat penetration within an ablating meteoroid. l is a scale size of an object—$r/3$ for a sphere, and K is the thermal conductivity of the meteoroid material.

It has been suggested that in most cases the rate of heat flow into a meteoroid would be such that the surface layers would be heated and ablated before the temperature of the core beneath is raised by any great extent (Podolak et al., 1988). In light of this, in order to allow the ablation of meteoroids larger than the commonly used isothermal cut-off of $\sim$1 mm to be modelled, we introduce a pseudo-thermal ablation mechanism. Using a similar technique to L&B91, an estimate of the depth to which a meteoroid may be assumed to be isothermal is made using Eq. (5). L&B91 calculate the heat transfer term, h of Eq. (5), using $h = \sigma T_{\rm s}^3$ and adopt an upper Biot number limit for isothermality of 0.1 (Kakaç and Yener, 1985; Incropera and DeWitt, 1996). Here $T_{\rm s}$ denotes the surface temperature of the meteoroid and therefore the temperature of the meteoroid's isothermal surface layer. Using the above expression for h, $r/3$ for l, and 0.1 for Bi we can rearrange Eq. (5) to give an expression for the depth of isothermal heat penetration into a meteoroid $\delta_{\rm iso}$, for a given surface temperature:

$$\delta_{\rm iso} = 0.3\frac{K}{\sigma T_{\rm s}^3}. \tag{6}$$

At each stage in the ablation process, this quantity is calculated using the current meteoroid surface temperature and subsequently used to determine the continuing mass loss rate through the energy balance equation. The alteration that this technique requires of the ablation equations is minimal. In fact only Eq. (4) has to be altered, to allow for the fact that the input energy now heats the smaller mass of an isothermal surface shell rather than that of the entire meteoroid. Using

$r_i = r_o - \delta_{iso}$, Eq. (4) is rewritten as

$$\frac{dT_s}{dt} = \left(\frac{4}{3}\pi\left(r_o^3 - r_i^3\right)\rho_m c\right)^{-1}\left(\frac{\Lambda}{2}\pi r_o^2 \rho_a v^3 + \pi r_o^2 S(1-\alpha) - 4\pi r_o^2 \epsilon_{rad}\sigma\left(T_s^4 - T_a^4\right) + L\frac{dm}{dt}\right), \quad (7)$$

where r_i and r_o are the inner and outer radii of the estimated isothermal shell, respectively.

Throughout this work we will assume a spherical symmetry for our ablating meteoroid. It has been shown that such an assumption is justified based on the rotational characteristics of meteoroids in the Earth's atmosphere. Öpik (1958) concluded that compact meteoroids and dust particles are likely to rotate and oscillate fast enough to justify approximating their average shape to that of a sphere (see also, Hawkes and Jones, 1978).

2.2.2. *Mass loss equation*

The goal of solving the ablation equations is to determine the rate at which mass is lost from a body during its interaction with an atmosphere. Knowledge of this quantity allows the determination of a meteor's luminosity and subsequently its magnitude. Here we will only consider mass loss due to vaporisation, ignoring any that may be due to sputtering of molecules from the surface which, it has been indicated, is only significant for very small (∼10 μm), very fast (∼70 km/s) meteoroids (Hill et al., 2004; Coulson, 2002). In this work we will assume that the object ablates continually from the surface. Under such circumstances the vapour pressure controlled ablation rate is derived from the Knudsen–Langmuir formula (Ip, 1990):

$$\frac{dm}{dt} = -4\pi r_o^2 P_{vap}(T_m)\sqrt{\frac{\mu}{2\pi k T_m}}. \quad (8)$$

The control of the mass loss by the vapour pressure P_{vap}, replaces the specific melting and vaporisation points used by some authors (Pecina and Ceplecha, 1983; Ceplecha et al., 1998) and is more meaningful in the rarefied upper atmosphere where the meteoroid is effectively ablating into a near vacuum. The vapour pressure is calculated according to Clausius–Clapeyron equation (Bronshten, 1983), and may be written as

$$\log_{10} P_{vap} = A - \frac{B}{T_m}, \quad (9)$$

where the constants A and B are material dependent and values for which were taken from Podolak et al. (1988). Other terms in Eq. (8) include Boltzmann's constant, k and the average mass of ablated particles, μ taken in this study to be constant even though its value may decrease with increasing meteoroid temperature due to thermal decomposition.

2.2.3. *Deceleration equation*

In, 1884 Kleiber formulated an equation describing how a meteoroid slows down as it passes through the Earth's atmosphere—see Bronshten (1983) for a historical review. By appealing to the principle of conservation of momentum the loss in momentum of the meteoroid is shown to be proportional to the momentum of the intersected air mass, resulting in the expression

$$\frac{dv}{dt} = -\frac{3}{4}\frac{\Gamma\rho_a v^2}{\rho_m r_o} + g\cos\theta \quad (10)$$

for the deceleration of a meteoroid with time. Due to the high entry speeds of even the slowest meteoroids, the gravitational term on the right-hand side is negligible for all but the latest stages of the meteor flight—*if* anything survives. In this study planetary curvature will be neglected. In Eq. (10) Γ, the drag coefficient, is that fraction of the momentum of the oncoming air flow that is converted into deceleration of the meteoroid and which, in this study, will be held at a constant value of unity. Note that the Γ used here differs by a factor of 2 from the often used aerodynamic drag coefficient, commonly written as $c_D = 2\Gamma$ (Hood and Horanyi, 1991).

2.2.4. *Luminosity and magnitude equations*

Throughout the ablation process, liberated meteoric molecules and atoms interact with atmospheric constituents becoming excited, ionised and dissociated and in the process exciting, ionising and dissociating the atmospheric atoms and molecules themselves. It is the subsequent relaxation and recombination of these altered states that result in the observable meteor phenomenon (Bronshten, 1983; Jenniskens et al., 2002). Note that while meteoric emission accounts for the majority of the observed light, the contribution of atmospheric lines to a meteor's spectrum increases with meteor velocity (Borovička, 2001). In this work, compositional differences between the two planets' atmospheres are neglected.

As mentioned earlier, the simultaneous solution of Eqs. (3), (7), (8), and (10) allows the calculation of a meteor's brightness by the substitution of the ablation rate into

$$I = -\frac{\tau}{2}v^2\frac{dm}{dt}, \quad (11)$$

where τ, the luminosity coefficient, is the fraction of the kinetic energy of the ablated material that is converted into visible light. In the past it has usually been taken that τ is dependent on the instantaneous speed of the meteoroid according to the relation

$$\tau = \tau_0 v^n, \quad (12)$$

where τ_0 is constant and the exponent n has a value of either 1 (Whipple, 1938) or −1 (Öpik, 1958) depending on the structure and initial speed of the meteoroid (Bronshten, 1983; Adolfsson et al., 1996). Recently, however, a study of 22 bright meteors by ReVelle and Ceplecha (2001) produced the following empirical expression for the luminosity coefficient as a function of instantaneous speed and mass

$$\ln\tau = -2.338 + \ln v + 1.15\tanh(0.38\ln m),$$
$$v \leqslant 24.372\ \mathrm{km\,s^{-1}},$$

$$\ln\tau = -0.344 - 10.307\ln v + 9.78\ln^2 v - 3.0414\ln^3 v + 0.3213\ln^4 v + 1.15\tanh(0.38\ln m), \quad v > 24.372\ \mathrm{km\,s^{-1}}, \quad (13)$$

wherein τ is given in percent, v in km s^{-1}, and m in kg (see also, Bellot Rubio et al., 2002).These equations give a value for the luminosity coefficient of ∼2% in all cases modelled in this study. Finally, following Öpik (1958) we calculate the absolute or zenithal magnitude M_v of a meteor from

$$M_v = 24.3 - 2.5\log_{10} I_{\mathrm{cgs}}. \quad (14)$$

Note that I_{cgs} in the above equation is in cgs units and differs from that given by Eq. (11) by a factor of 10^7.

2.3. Atmospheric models

To model meteoroid ablation in the terrestrial atmosphere, atmospheric density and temperature values were calculated using the MSIS-E 90 model (Hedin, 1991). The values used were the default values for midnight on June 29th/30th at 0° latitude, 0° longitude. For Venus, density and temperature data tabulated by Seiff (1983), were interpolated at the required heights, using a cubic spline routine (Press et al., 1996). In relation to Seiff's model, for the altitude range 60–100 km where diurnal variations are small, data was used for latitudes of 0–30°, while for the 100–180 km range the data used corresponded to the midnight or antisolar point (solar elongation >120°).

2.4. Numerical integration

The ablation model was coded in Fortran 90. Eqs. (3), (8), and (10) of Section 2.2 and the reformulated Eq. (7) were numerically integrated using an adaptive Runge–Kutta–Fehlberg algorithm (Shampine and Watts, 1977), on a dual processor Intel Xeon system. This setup allowed large parameter batches to be simulated in a couple of hours, the extra computation time required for the adaptive stepping not proving inhibitive.

3. Results

Before we discuss the results of our simulations, we remind the reader that this is foremost a comparative study. It is reasonable to assume that, for identical particles ablating in two different atmospheres, the mechanisms of ablation are the same and that any differences in the meteors produced are mainly due to different temperature and density profiles (e.g., different scale heights) at the two planets' atmospheres. In all models of meteor ablation to-date, inherent uncertainties in meteoroid composition and bulk densities have proved to be one of the largest obstacles to accurate meteor simulation. However, assuming that the removal of these uncertainties from ablation models would affect meteor phenomena in a similar fashion in different atmospheres, we propose that the relative values of meteor brightness, heights of ablation, duration and trail lengths, presented here, would remain largely unchanged.

In this study we have not incorporated fragmentation mechanisms into our model, mechanisms which have been used to generate and fit synthetic light curves to many observed meteors (Jacchia, 1955; Öpik, 1958; Hawkes and Jones, 1975; Novikov, 1984; Campbell-Brown and Koschny, 2004). Single-body ablation models such as the one developed in this work, have however been shown to be capable of reproducing observed light curves (Bellot Rubio et al., 2002).

The relative values of brightness and ablation heights presented here for meteors at Venus are in reasonable agreement with recent analytical studies (Christou, 2004), and should give a good indication of what in situ studies might expect to observe of meteors at Venus. The differences between the numerical results of this work and Christou's analytic estimates are attributed to two main factors. Firstly that author uses simple exponential atmospheres with constant scale heights at each planet, as opposed to the interpolated atmospheric models used in our simulations. Also, the expression used by Christou to determine relative brightnesses of terrestrial and venusian meteors (Eq. (2), Christou, 2004) is based on that derived by Adolfsson et al. (1996) in which both heat conduction and radiative cooling are neglected.

3.1. Comparison with observation

As well as agreeing with analytical predictions for Venus, a reliable model should also be in reasonable agreement with what is observed of meteors at the Earth. To this end, Table 2 compares the results of the simulation of both rocky (3.4 g cm^{-3}) and icy (1.0 g cm^{-3}) meteors using our model with the observational data for 496 meteors from five dif-

Table 2
Simulated and observational maximum magnitude comparison

Meteor shower (v_g [km s^{-1}][a])	Mass range ($\log_{10} M_p$ [g])	Maximum magnitudes		
		Koten et al. (2004)	Ice[a]	Rock[b]
Leonids (70.7)	−3.68 → −1.82	−0.3 → 3.4	−1.8 → 4.2	−1.8 → 2.8
Orionids (66.4)	−3.82 → −1.77	−1.0 → 3.8	−1.6 → 4.0	−1.5 → 3.1
Perseids (59.6)	−4.00 → −1.03	−2.1 → 4.2	−3.7 → 4.4	−3.3 → 3.6
Geminids (34.4)	−3.17 → −0.80	−0.3 → 4.6	−1.3 → 3.7	−1.2 → 3.5
S. Taurids (27.0)	−2.82 → −0.96	0.8 → 4.7	−0.3 → 4.7	−0.2 → 4.5

The above values show the agreement between our simulated meteors and the observational data tabulated by Koten et al. (2004) for five prominent showers. In all cases, the maximum magnitudes for the specified mass ranges agree to within ∼1.6 mag.

[a] v_g, geocentric velocities taken from Cook (1973).

[b] Values as determined in this paper for ice (1.0 g cm^{-3}) and rock (3.4 g cm^{-3}).

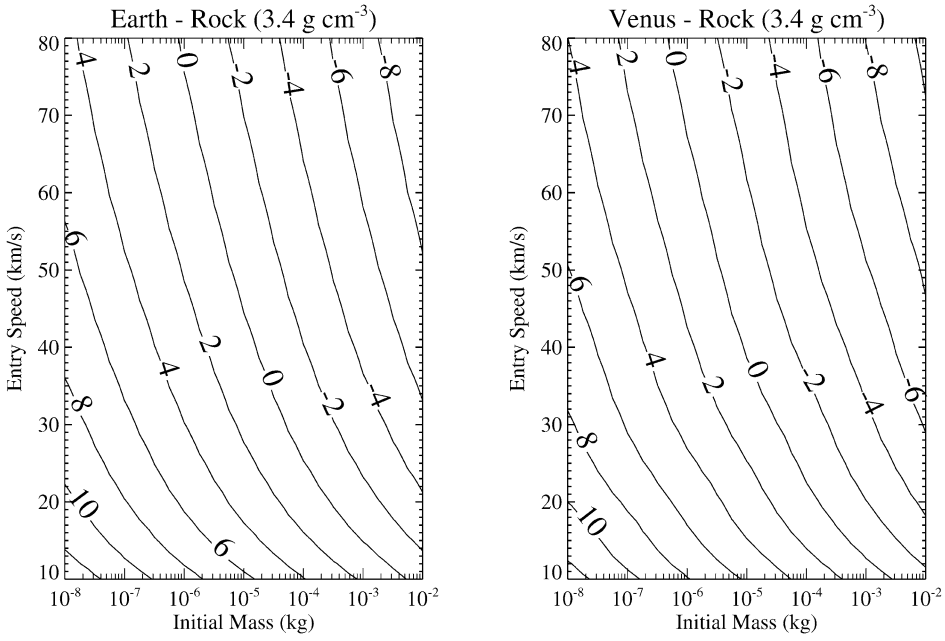

Fig. 1. Maximum magnitude reached during ablation of rocky material (3.4 g cm^{-3}) in the terrestrial (left) and venusian (right) atmospheres.

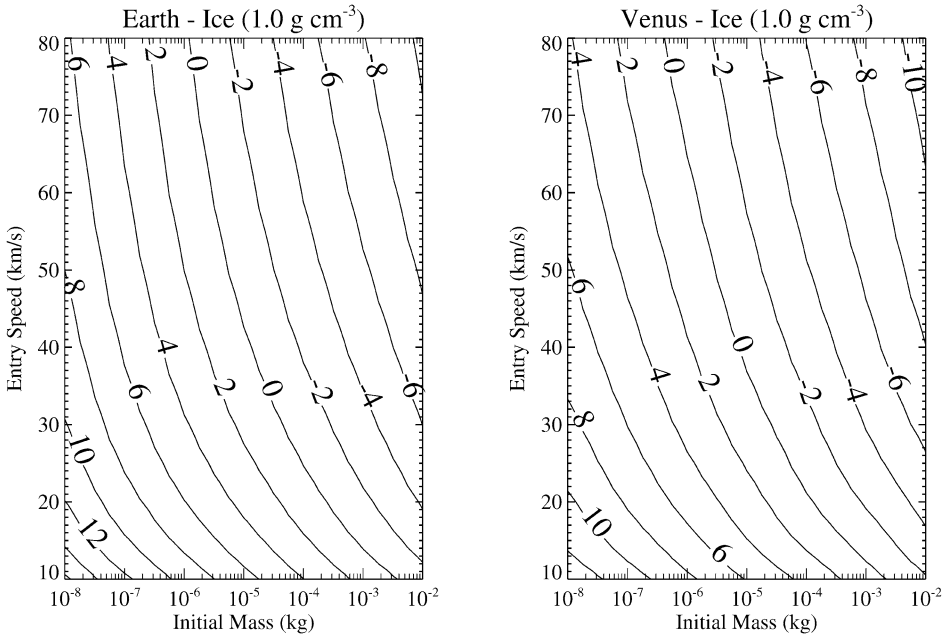

Fig. 2. Maximum magnitude reached during ablation of icy material (1.0 g cm^{-3}) in the terrestrial (left) and venusian (right) atmospheres.

ferent showers tabulated by Koten et al. (2004). The mass ranges used in these simulations, and shown in Table 2, are listed in Table 1 of Koten et al. (2004). In all cases, the maximum magnitudes for the specified mass ranges agree to within 1.6 mag.

3.2. Brightnesses and relative brightness

As previously mentioned, due to the inherent uncertainties in meteoroid composition, this study uses the material characteristics of water ice and chondritic stone, to model and compare terrestrial and venusian meteors. In both material cases, on both planets, it is seen that the maximum magnitude (MM) reached during ablation increases with increasing initial velocity and initial mass, see Figs. 1 and 2—bigger and faster meteoroids produce brighter meteors. With reference to Eq. (7), an increase in the initial velocity and/or mass (and therefore radius), results in an increase in the collisional energy input, or Λ-term, on the right-hand side. Thus, for faster, larger bodies more energy is available for ablation of the meteoroid resulting in brighter meteors on both planets.

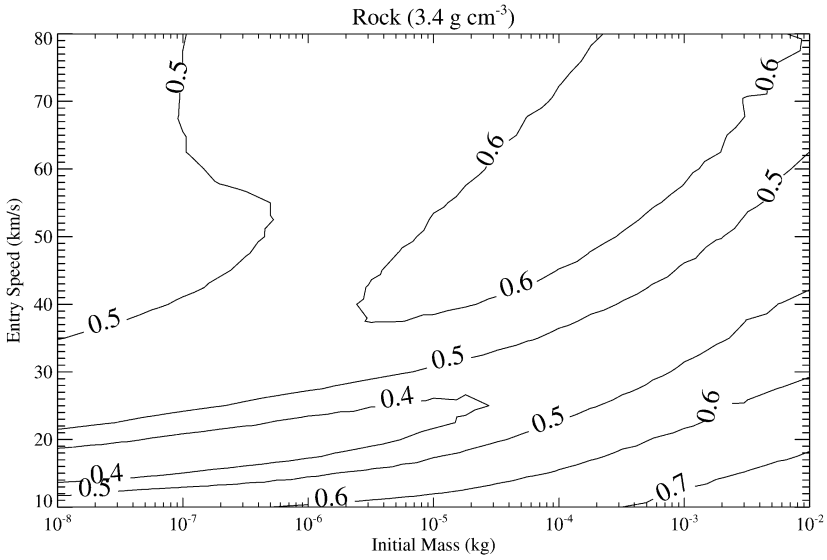

Fig. 3. Difference in maximum magnitudes reached during ablation of rocky material (3.4 g cm^{-3}) at the Earth and Venus (Earth minus Venus).

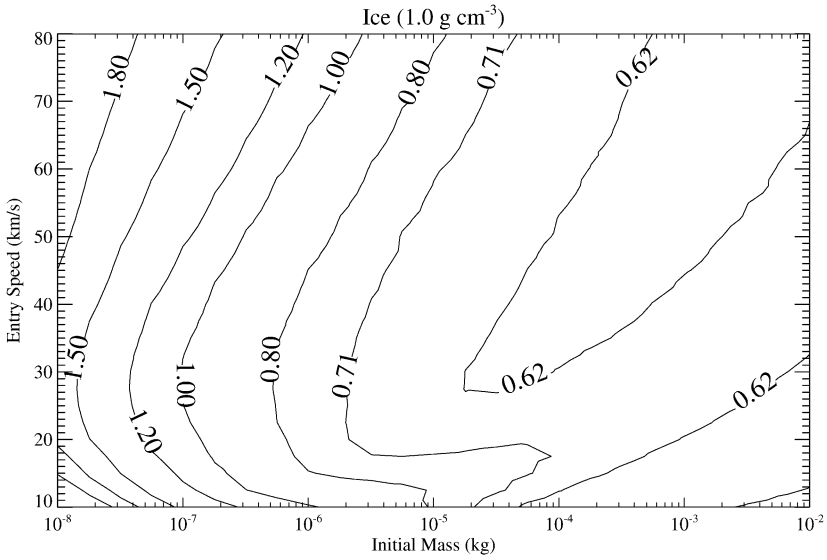

Fig. 4. Difference in maximum magnitudes reached during ablation of icy material (1.0 g cm^{-3}) at the Earth and Venus (Earth minus Venus).

Comparing the MM of the two materials on the two planets it is found that, for dense rocky particles (Fig. 3), the greatest MM differences occur for large slow objects. In the case of icy cometary meteoroids (Fig. 4), the relative difference of the MM at the two planets is largest for low mass objects with moderate to high entry velocities, (30–60 km s^{-1}). In all velocity and mass cases modelled, venusian meteors both rocky and icy, are as bright as, if not brighter than, terrestrial meteors given the same initial conditions. For rocky objects larger than 10^{-3} kg entering with velocities less than 20 km s^{-1} this difference is upwards of 0.6 mag. For icy particles, differences of 1.7–2.0 mag are found for low mass ($\sim 10^{-8}$ kg) particles. At the Earth, the meteoroid mass distribution skews toward the low mass end of the spectrum, resulting in greater numbers of fainter meteors. The above results, for low mass, average speed meteors at Venus, suggest that the detection rates for MSX-type observations[1] (Jenniskens et al., 2000) would be significantly enhanced.

3.3. *Heights of peak brightness*

The height at which a meteor reaches its MM is also dependent on initial mass, velocity and zenith angle, as well as on the composition of the ablating body. As commonly known, upon atmospheric entry, the more massive a body is for a given speed, the deeper or lower down will be its point of maximum brightness. Perhaps not so intuitive is that for a

[1] The Midcourse Space Experiment (MSX) was launched on April 24, 1996. It had a unique ability for both space-based meteor imaging and UV spectroscopy over a wide spectral range. See Jenniskens et al. (2002).

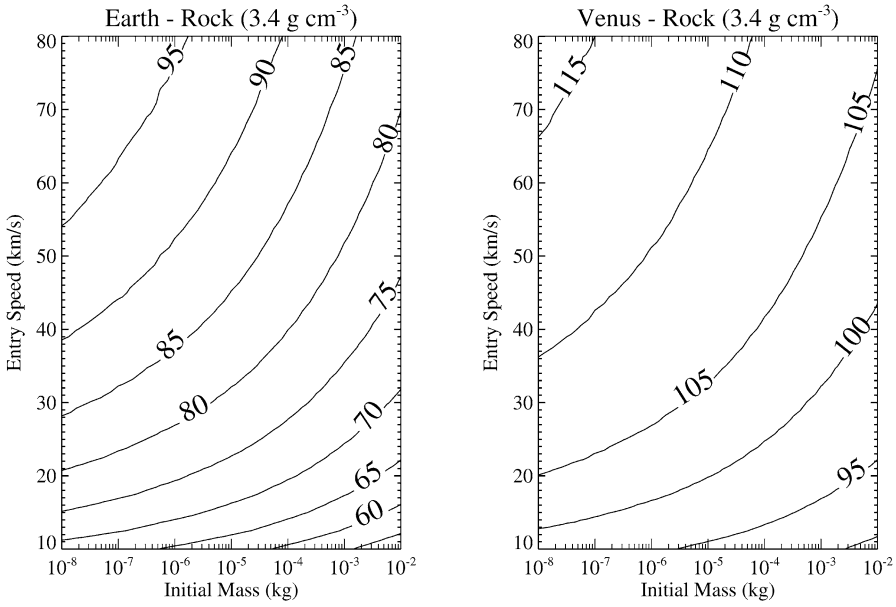

Fig. 5. Height (km) of maximum magnitude reached during ablation of rocky material (3.4 g cm^{-3}) in the terrestrial (left) and venusian (right) atmospheres.

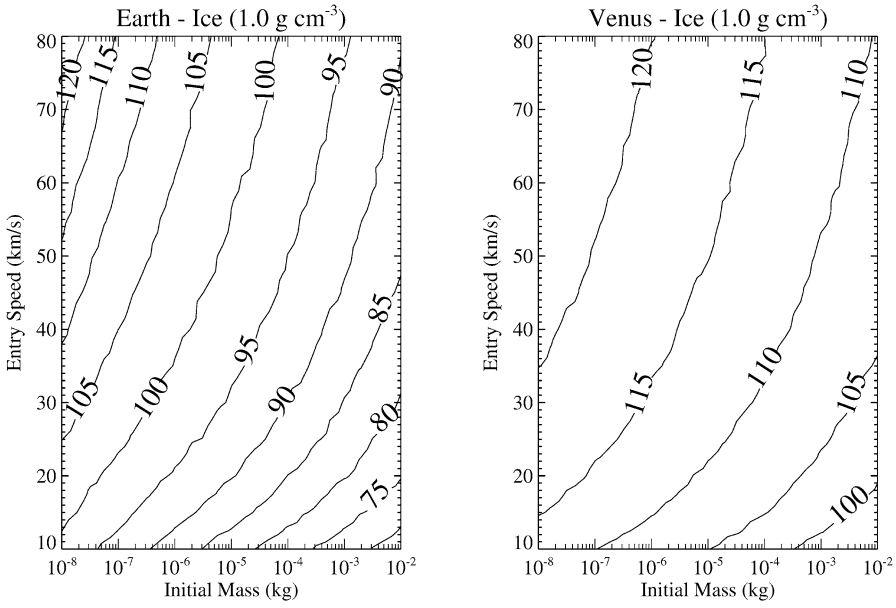

Fig. 6. Height (km) maximum magnitude reached during ablation of icy material (1.0 g cm^{-3}) in the terrestrial (left) and venusian (right) atmospheres

fixed mass, the height of MM increases with increasing entry speed. Faster objects ablate more aggressively due to the input energy's cubic dependence on velocity (see Eq. (8)). This more rapid mass loss dominates over the higher entry speed, resulting in maximum brightness earlier, or at greater altitude. Inspection of Figs. 5 and 6 shows these behaviours to hold for both materials modelled for both planets. It can also be seen that the more friable icy bodies ablate faster than their rocky counterparts and so reach MM higher up.

The sweeping shape of the contours in Figs. 5 and 6 also indicates that the height of MM becomes less dependent on mass and more dependent on velocity as the mass decreases and vice versa. This mass independence of MM heights for small particles was noted by Koten et al. (2004) in reference to Hawkes and Jones' (1975) dust-ball model. The MM height comparison plots of Figs. 7 and 8, for rock and ice, respectively, show agreement with Christou's (2004) analytical study of venusian meteors. Christou gives a venusian ablation range of 100–120 km, some 20–30 km higher than at the Earth. Figs. 7 and 8 agree, indicating that the height differences are greatest for large slow particles and that, on the whole, are greater for rocky bodies than for icy meteoroids.

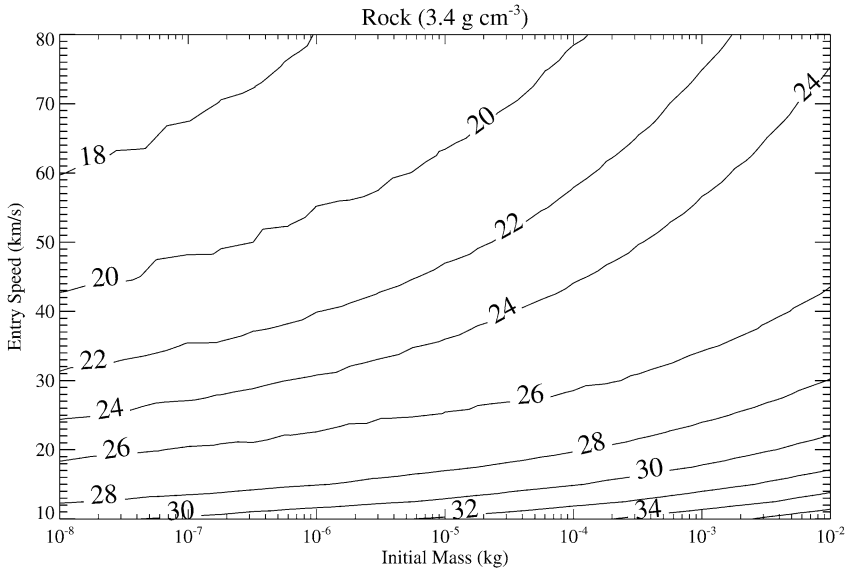

Fig. 7. Difference in heights (km) of maximum magnitude reached during ablation of rocky material (3.4 g cm^{-3}) at the Earth and Venus (Venus minus Earth).

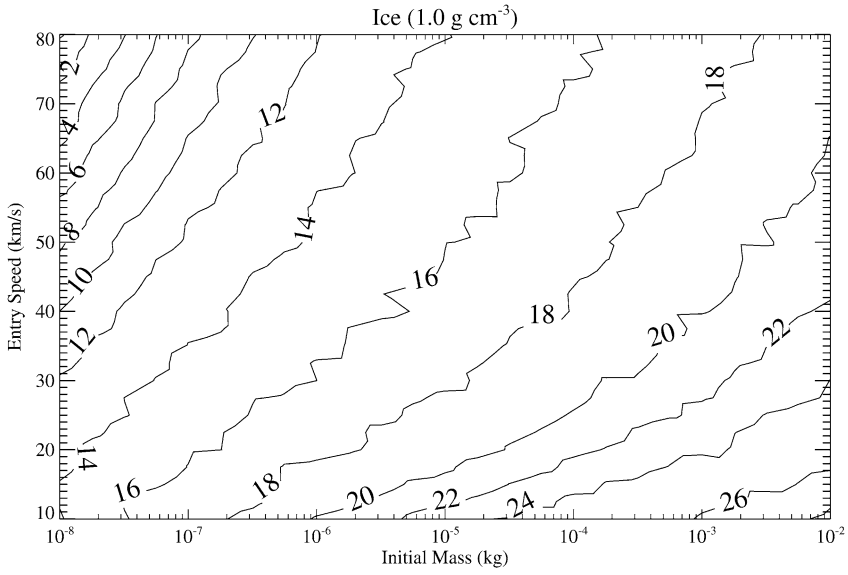

Fig. 8. Difference in heights (km) of maximum magnitude reached during ablation of icy material (1.0 g cm^{-3}) at the Earth and Venus (Venus minus Earth).

The fact that venusian meteors ablate at the altitudes suggested by Figs. 5 and 6 bodies well for future in situ observational campaigns as these altitudes are well above the haze/cloud decks of the lower venusian atmosphere (Prinn and Fegley, 1987).

The coarseness of some of the contours in Figs. 8–14 is due to the resolution of the mass-speed grid used in the simulation. Nevertheless their general shape and behaviour is sufficient to convey the overall changes in parameters' values with respect to initial mass and speed.

3.4. Duration of visibility and trail length

Estimates of the expected periods for which meteors are visible and the lengths of their visible trails are useful in designing and building observational apparatus. In skyward looking setups (in the case of the Earth) or orbiting systems looking at a planet's limb (as may be employed at both planets), too long exposure times would result in CCD saturation due to atmospheric airglow (Christou, 2004) and in a possible loss of meteor data. In this study +6.5 mag was taken as a *dimmer* limit of observability and for those meteors with maximum brightnesses above this cut-off the duration of visibility, as well as each meteor's trail length, was calculated.

The four plots of Figs. 9 and 10 show the calculated visibility times for icy and rocky particles, respectively, at the Earth and Venus. Of those meteors that become visible ($M_{V_{\max}} \leqslant +6.5$) it is evident that large slow particles remain visible longest. The general shape of all four plots changes

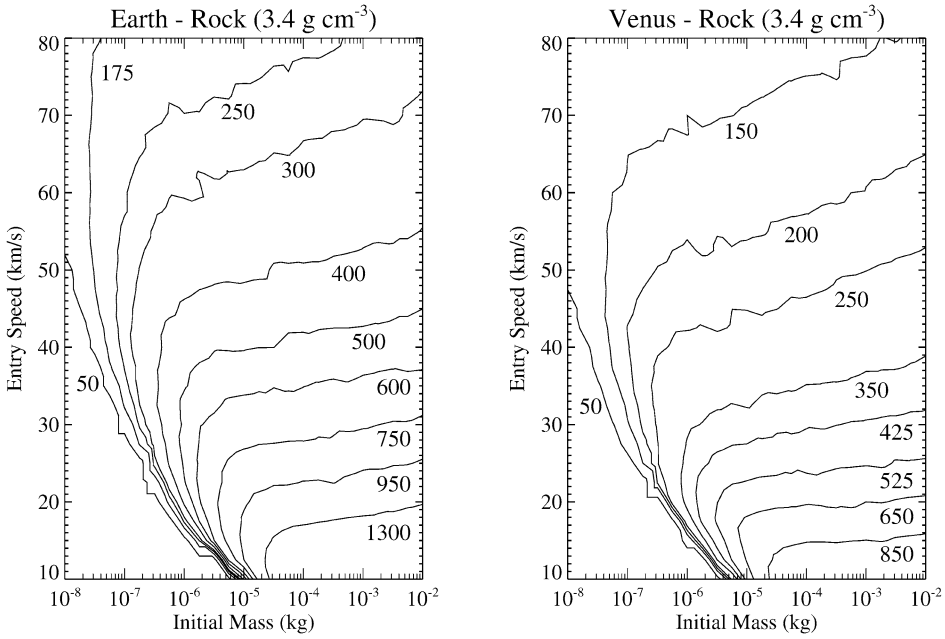

Fig. 9. Duration of visibility (ms) of ablating rocky meteoroid (3.4 g cm^{-3}) in the terrestrial (left) and venusian (right) atmospheres (in all cases duration of visibility is the period of time for which the magnitude of the meteor is less that +6.5).

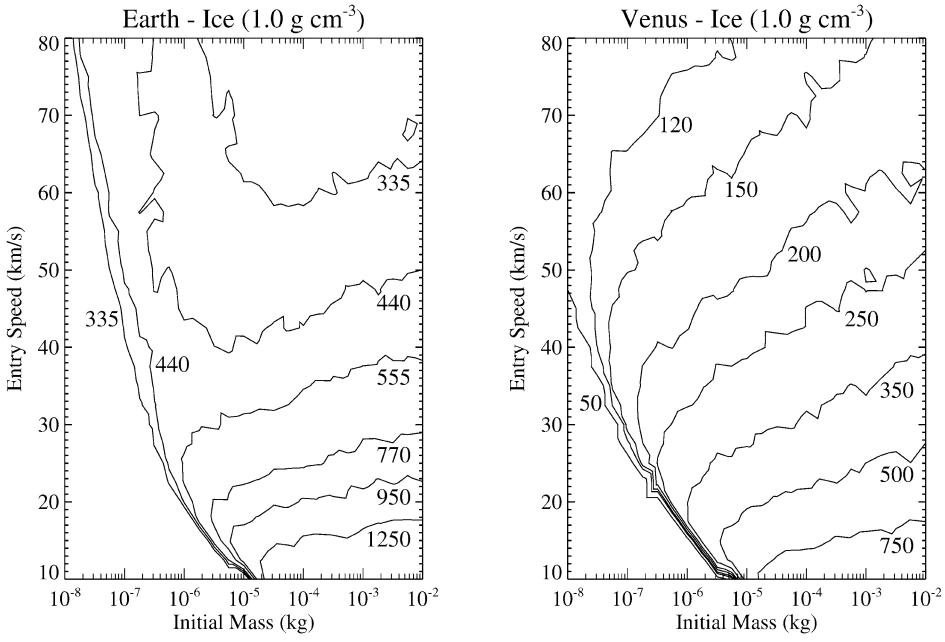

Fig. 10. Duration of visibility (ms) of ablating icy meteoroid (1.0 g cm^{-3}) in the terrestrial (left) and venusian (right) atmospheres.

in a similar manner, indicating that small fast particles are the shortest lived. The plateau feature in the Earth plot of Fig. 10 suggests that visibility times become less dependent on changes in initial velocity and mass as both these parameters increase. This feature was also seen for theoretical icy particles at Venus with initial velocities greater than those physically possible for Sun-bound material near 0.72 AU. Though not shown here, visibility time studies with a varying zenith angle show that the duration of visibility of a given meteor increases with increasing entry angle. All cases shown in this work correspond to an entry angle of 45°.

As can be seen in Figs. 9 and 10, visibility times for rock are greater than those for ice on both planets—rocky meteors last longer. For the mass and velocity ranges modelled in this work there may be up to 1.5 s between the points of appearance and disappearance of a dense rocky meteoroid at the Earth, and up to 0.9 s for the same meteor at Venus. For the most part, meteors at the Earth tend to remain visible for up to twice or three times as long as similar meteors on Venus

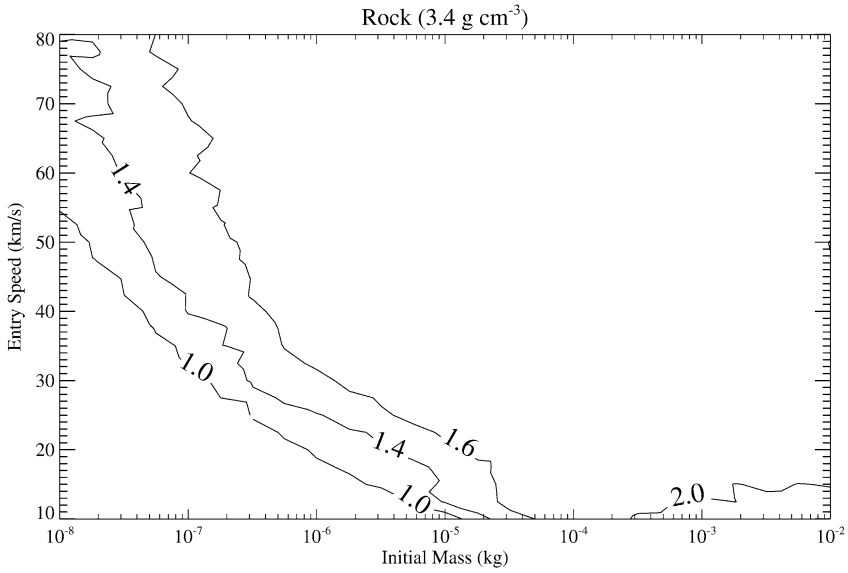

Fig. 11. Ratio of terrestrial visibility time to venusian visibility time for rocky particles (3.4 g cm^{-3}—Earth/Venus).

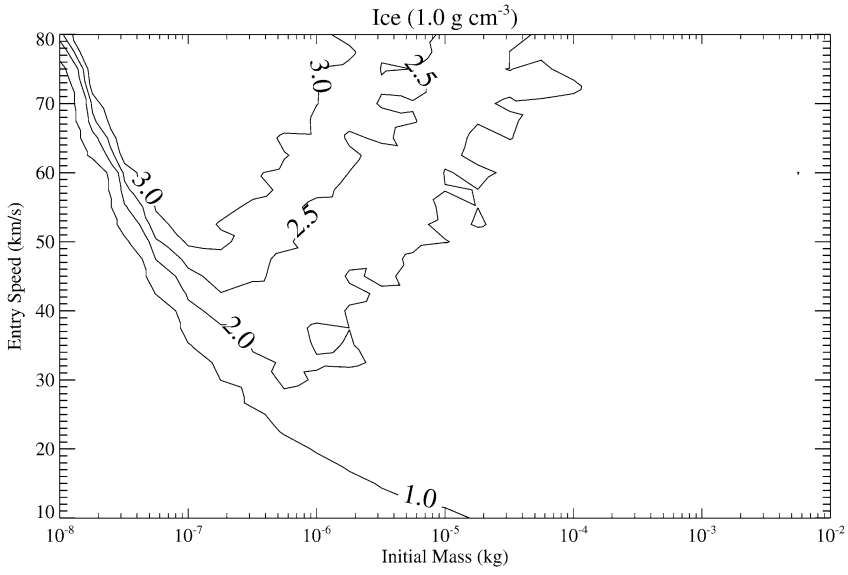

Fig. 12. Ratio of terrestrial visibility time to venusian visibility time for icy particles (1.0 g cm^{-3}—Earth/Venus).

(see Figs. 11 and 12), due mainly to the shorter venusian atmospheric scale height (Christou, 2004). This shorter scale height causes venusian meteors to ablate more aggressively and therefore more quickly than their terrestrial equivalents, resulting in shorter meteor visibility times and consequently shorter meteor trails at Venus. It can be seen from Figs. 13 and 14 that the ratios of meteor trail lengths between the two planets correspond to the visibility time ratios of Figs. 11 and 12, with venusian meteors having, on average, between 20 and 30% shorter trail lengths than their terrestrial equivalents. As the limit of visibility is neared for both materials, the 1.0-line in Figs. 11 and 12 is crossed from right to left, suggesting that the faintest of venusian meteors, far too faint to be detected visually, last for up to twice as long as similar particles at the Earth.

3.5. *Differences for particular showers*

The results of the above sections were obtained by comparing identical objects ablating in two different atmospheres. In reality, however, meteoroid streams associated with a particular parent body will encounter the Earth and Venus at different speeds—*similar* to the close approach speeds of the parent bodies themselves.[2] Using an analytical

[2] Small differences will exist between the speed of a comet/asteroid at its closest approach to a planet and the speed at which its meteoroid stream (if one exists) encounters that planet's atmosphere. Such differences will be due to the meteoroids having been ejected from the parent body with a distribution of velocities as well as gravitational perturbations along the orbit.

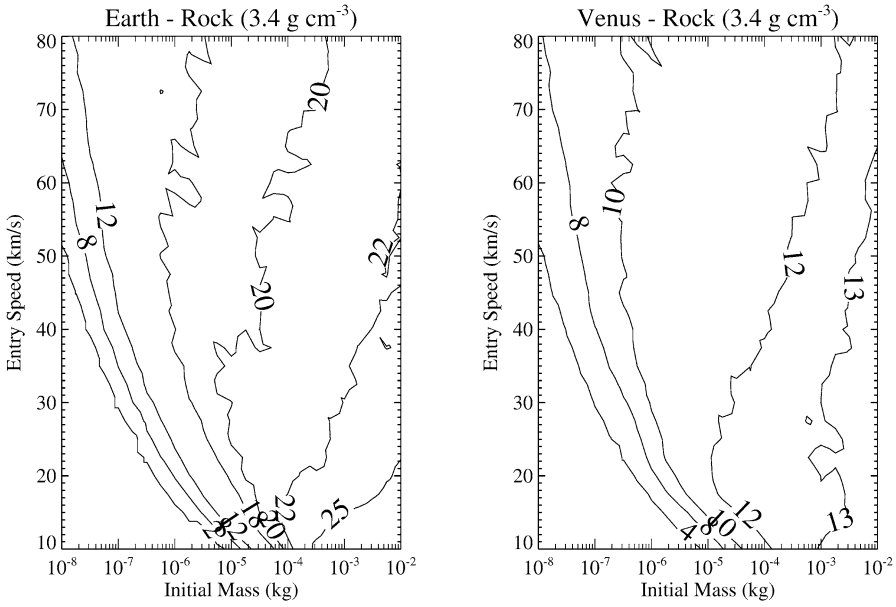

Fig. 13. Meteor trail lengths for rocky particles (3.4 g cm^{-3}) in the terrestrial (left) and venusian (right) atmospheres.

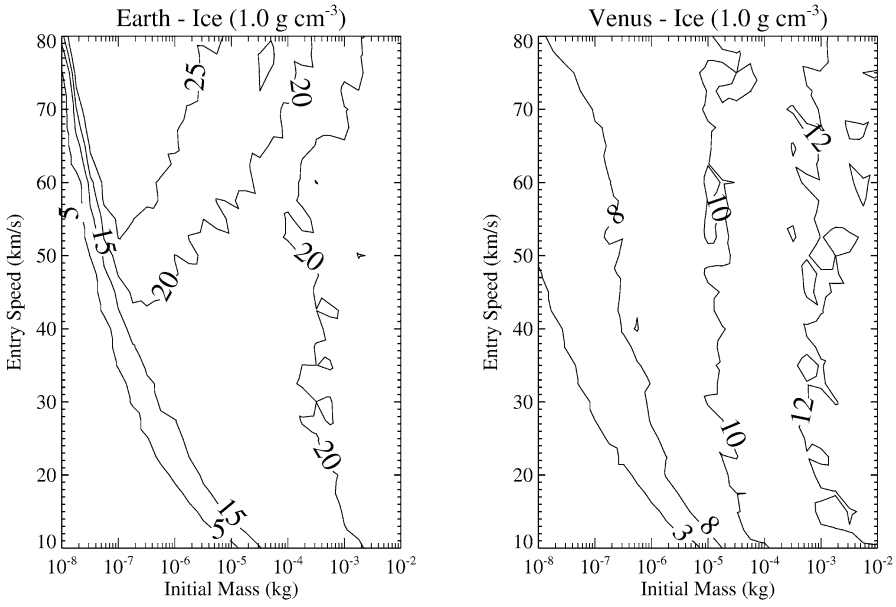

Fig. 14. Meteor trail lengths for icy particles (1.0 g cm^{-3}) in the terrestrial (left) and venusian (right) atmospheres.

technique developed by Adolfsson et al. (1996) to estimate the relative brightness of martian meteors with respect to meteors at the Earth, Christou (2004) calculated the likely brightness differences between venusian and terrestrial meteors associated with Halley type comet (HTC) 1P/Halley, Jupiter family comet (JFC) 45P/Honda–Mrkos–Pajdusakova and the cometary Asteroid 3200 Phaethon. In the same work Christou determined these objects, known to pass close to the Earth and believed to produce annual meteor showers in its atmosphere, to also pass close enough to Venus as to possibly result in significant and observable meteor activity in its atmosphere.

Table 3 shows the maximum magnitudes, heights of maximum magnitudes and durations of visibility of meteors associated with these three objects at the Earth and at Venus. Christou estimates venusian Halleyids (which, on Venus, would be Picids) to be 0.7 mag greater than their terrestrial cousins—less than half the value resulting from our numerical simulations, which suggest that venusian Halleyids of 5.6×10^{-6} kg, would be 1.5 mag brighter than Halleyids at the Earth (Eta Aquarids—Lindblad et al., 1994; Orionids—Hughes, 1987). In the case of the Asteroid 3200 Phaethon, associated with the December Geminids at the Earth (Whipple, 1983; Williams and Wu, 1993) Christou

Table 3
Meteor parent body comparison

Parent body Planet	Maximum magnitude	Height of MM (km)	Duration (s)
	1P/Halley		
Earth (67.0 km s^{-1})	−1.3	102.5	0.4
Venus (80.0 km s^{-1})	−2.8	118.2	0.1
	3200 Phaethon		
Earth (36.0 km s^{-1})	1.5	82.4	0.6
Venus (42.0 km s^{-1})	0.2	107.2	0.3
	45P/Honda–Mrkos–Pajdusakova		
Earth (27.0 km s^{-1})	2.7	94.5	0.6
Venus (25.0 km s^{-1})	2.4	111.8	0.4

The above values correspond to meteoroids of initial mass 5.6×10^{-6} kg. The bracketed values following each planet's name represent the encounter velocity of the relevant parent body with that planet (Christou, 2004).

determines venusian meteors to be brighter, this time by 0.7–1.0 mag. Our simulations also show venusian Geminids[3] to be brighter but give a difference of 1.3 mag. Finally, for Comet 25P/Honda–Mrkos–Pajdusakova, which has been linked to August's α Capricornids at the Earth (Hasegawa, 1990) and would also appear to radiate from Capricornus at Venus (Christou, 2004), we find that its meteors at Venus are again the brighter, with a difference of 0.3 mag compared to a range of 0.15–0.25 given by Christou. While in reasonable agreement, the above differences between our numerical results and Christou's estimates, are mainly attributed to the factors discussed previously in the opening paragraphs of Section 3.

Also given in Table 3 are the heights at which the meteors reach the point of maximum brightness. As predicted, meteors associated with these three parent bodies would reach maximum brightness some 15–25 km higher up in the venusian atmosphere than at the Earth. We also see that the lengths of time for which these venusian meteors should be visible agree with the general results of Section 3.4, in that they are shorter lived than equivalent terrestrial meteors, but still of sufficient duration to be detectable using current and future observational technologies.

4. Conclusions and future work

This paper has sought to corroborate the findings of Christou's (2004) analytical study of venusian meteor brightness and ablation heights, through numerical simulation. Extending the classical single-body ablation model to allow for some differential heating, icy and rocky meteoroids of up to 10^{-2} kg (equivalent to ∼8 mm initial radius for rock and ∼13 mm for ice) were simulated ablating in the terrestrial and venusian atmospheres.

Comparisons of maximum magnitudes, the heights at which these were reached, and the duration of meteor visibility, as well as meteor trail length, were carried out. In general, venusian meteors tend to be as bright as, if not brighter than, meteors in the terrestrial atmosphere due to the shorter atmospheric scale height at Venus. Upon atmospheric entry venusian meteors effectively hit a wall of air while terrestrial meteors experience a softer cushioning effect. Large (∼10^{-2} kg), slow (∼20 km s^{-1}), rocky objects were found to be up to ∼0.7 mag brighter on Venus, while small (⩽10^{-8} kg) icy particles with moderate entry speeds (∼30–60 km s^{-1}) were shown to be ∼2.7 mag brighter than at the Earth. Our simulations also indicate that venusian meteors reach their points of maximum ablation, and therefore maximum magnitude, at greater heights than would identical objects ablating at the Earth. The height differences calculated correspond to the intrinsic differences in the two planets' atmospheric density profiles, such that, although the height intervals over which maximum brightness is reached differ from planet to planet the atmospheric density intervals are similar (see Fig. 1, Christou, 2004). For the initial velocity and mass ranges modelled here, rocky meteoroids reach maximum brightness some 15–35 km higher up at Venus, while for icy particles this altitude difference is 5–25 km.

Venusian meteors tend, in general, to be shorter lived than terrestrial meteors, again due to the shorter scale height of the venusian atmosphere—that which burns brightest, burns quickest. In terms of absolute visibility times, of those meteors that become brighter than +6.5 mag, most remain visible for several hundreds of milliseconds, with the largest, slowest particles modelled remaining visible for almost one second at Venus. With such periods of visibility expected, space-based observations similar to that of the MSX spacecraft reported by Jenniskens et al. (2000), should be capable of in situ orbital detection. Absolute meteor trail lengths at Venus were also found to be up to half those calculated for similar particles at the Earth, in agreement with our findings for meteor visibility times.

With a view to studying how meteoroid streams with probable associations to known parent bodies, might differ in the way they ablate in the atmospheres of different planets, meteors linked to 2 comets and 1 cometary asteroid (1P/Halley, 45P/Honda–Mrkos–Pajdusakova, 3200 Phaethon) were simulated. It was found that venusian meteors were brighter in all cases. The greatest differences for the materials modelled were found for HTC with venusian Halleyids being 1.5 mag brighter than their terrestrial equivalents.

As the model used in this work is based on the classical single-body ablation equations, future work should look at incorporating a fragmentation mechanism such as that of Campbell-Brown and Koschny (2004). Many of the techniques developed for modelling meteoroid stream evolution

[3] A meteor shower linked with 3200 Phaethon at Venus would have a radiant on the border of the constellations Gemini and Lynx (Christou, 2004).

(and consequently meteor shower activity), in the past few years (McNaught and Asher, 1999; Vaubaillon and Colas, 2002), could be applied to determining the meteoroid flux density at Venus, allowing any future observational campaigns to be optimised. Also, a more sophisticated venusian atmosphere model such as the VIRA empirical model could be incorporated.

Acknowledgments

Astronomical research at Armagh Observatory is funded by The Northern Ireland Department of Culture, Arts and Leisure. The authors thank David Asher for his comments on early drafts of the manuscript, Youra Taroyan for his translation of Russian papers, and Chris Trayner for help with the theoretical model in its early stages; Detlef Koschny and Joseph M. Grebowsky for suggestions which improved the paper in its final version.

References

Adolfsson, L.G., Gustafson, B.A.S., Murray, C.D., 1996. The martian atmosphere as a meteoroid detector. Icarus 119, 144–152.

Apshtein, E.Z., Piliugin, N.N., Vartanian, N.V., 1982. Investigation of meteor ablation in the atmospheres of the Earth, Mars, and Venus. Kosm. Issledov. 20, 730–735. In Russian.

Baggaley, W.J., Marsh, S.H., Bennett, R.G.T., Galligan, D.P., 2001. Features of the enhanced AMOR facility: The Advanced Meteor Orbit Radar. In: Proc. Meteoroids 2001 Conf., pp. 387–391.

Beech, M., 1998. Venus-intercepting meteoroid streams. Mon. Not. R. Astron. Soc. 294, 259–263.

Bellot Rubio, L.R., Martínez González, M.J., Ruiz Herrera, L., Licandro, J., Martínez Delgado, D., Rodríguez Gil, P., Serra-Ricart, M., 2002. Modelling the photometric and dynamical behaviour of super-Schmidt meteors in the Earth's atmosphere. Astron. Astrophys. 389, 680–691.

Borovička, J., 2001. Video spectra of Leonids and other meteors. In: Proc. Meteoroids 2001 Conf., pp. 203–208.

Bronshten, V.A., 1983. Physics of Meteoric Phenomena. Reidel, Dordrecht.

Campbell-Brown, M.D., Koschny, D., 2004. Model of the ablation of faint meteors. Astron. Astrophys. 418, 751–758.

Ceplecha, Z., Borovička, J., Elford, W.G., Revelle, D.O., Hawkes, R.L., Porubčan, V., Šimek, M., 1998. Meteor phenomena and bodies. Space Sci. Rev. 84, 327–471.

Ceplecha, Z., Borovička, J., Spurný, P., 2000. Dynamical behaviour of meteoroids in the atmosphere derived from very precise photographic records. Astron. Astrophys. 357, 1115–1122.

Christou, A.A., 2004. Prospects for meteor shower activity in the venusian atmosphere. Icarus 168, 23–33.

Cook, A.F., 1973. A working list of meteor streams. NASA SP 319, 183.

Coulson, S.G., 2002. Resistance of motion to a small, hypervelocity sphere, sputtering through a gas. Mon. Not. R. Astron. Soc. 332, 741–744.

Davis, P.M., 1993. Meteoroid impacts as seismic sources on Mars. Icarus 105, 469–478.

Flynn, G.J., McKay, D.S., 1990. An assessment of the meteoritic contribution to the martian soil. J. Geophys. Res. 95, 14497–14509.

Grebowsky, J.M., 1981. Meteoric ion production near Jupiter. J. Geophys. Res. 86, 1537–1543.

Hasegawa, I., 1990. Predictions of the meteor radiant point associated with a comet. Publ. Astron. Soc. Jpn. 42, 175–186.

Hawkes, R.L., Jones, J., 1975. A quantitative model for the ablation of dustball meteors. Mon. Not. R. Astron. Soc. 173, 339–356.

Hawkes, R.L., Jones, J., 1978. The effect of rotation on the initial radius of meteor trains. Mon. Not. R. Astron. Soc. 185, 727–734.

Hedin, A., 1991. Extension of the MSIS thermosphere model into the middle and lower atmosphere. J. Geophys. Res. 96, 1154–1172.

Hill, K.A., Rogers, L.A., Hawkes, R.L., 2004. Significance of sputtering in meteoroid ablation. In: Meteoroids 2004, Ses. 6, Abs. 2. Abstract.

Hood, L.L., Horanyi, M., 1991. Gas dynamic heating of chondrule precursor grains in the solar nebula. Icarus 93, 259–269.

Hughes, D.W., 1987. P/Halley dust characteristics—A comparison between Orionid and Eta Aquarid meteor observations and those from the flyby spacecraft. Astron. Astrophys. 187, 879–888.

Hunten, D.H., Turco, R.P., Toon, O.B., 1980. Smoke and dust particles of interplanetary origin in the mesosphere and stratosphere. J. Atmos. Sci. 37, 1342–1357.

Incropera, F.P., DeWitt, D.P., 1996. Fundamentals of Heat and Mass Transfer, fourth ed. Wiley, New York.

Ip, W.H., 1990. Meteoroid ablation processes in Titan's atmosphere. Nature 345, 511–512.

Jacchia, L.G., 1955. The physical theory of meteors. VIII. Fragmentation as a cause of the faint-meteor anomaly. Astrophys. J. 121, 521–527.

Jenniskens, P., 2001. Meteors as a delivery vehicle for organic matter to the early Earth. In: Proc. Meteoroids 2001 Conf., pp. 247–254.

Jenniskens, P., Nugent, D., Tedesco, E., Muthry, J., 2000. 1997 Leonid shower from space. Earth Moon Planets 82–83, 305–312.

Jenniskens, P., Tedesco, E., Muthry, J., Laux, C.O., Price, S., 2002. Space-borne ultraviolet 251–384 nm spectroscopy of a meteor during the 1997 Leonid shower. Meteorit. Planet. Sci. 37, 1071–1078.

Kakaç, S., Yener, Y., 1985. Heat Conduction. Hemisphere, New York.

Kim, Y.H., Pesnell, W.D., Grebowsky, J.M., Fox, J.L., 2001. Meteoric ions in the ionosphere of Jupiter. Icarus 150, 261–278.

Koten, P., Borovička, J., Spurný, P., Betlem, H., Evans, S., 2004. Atmospheric trajectories and light curves of shower meteors. Astron. Astrophys. 428, 683–690.

Lindblad, B.A., 2001. IAU Meteor Data Center. In: Proc. Meteoroids 2001 Conf., pp. 71–72.

Lindblad, B.A., Ohtsuka, K., Shirakawa, K., 1994. The orbit of the Eta Aquarid meteor stream. Planet. Space Sci. 42, 113–116.

Love, S.G., Brownlee, D.E., 1991. Heating and thermal transformation of micrometeoroids entering the Earth's atmosphere. Icarus 89, 26–43.

McNaught, R.H., Asher, D.J., 1999. Leonid dust trails and meteor storms. J. Int. Meteor Org. 27, 85–102.

Moses, J.I., 1992. Meteoroid ablation in Neptune's atmosphere. Icarus 99, 368–383.

Novikov, G.G., 1984. The fragmentation of meteoroids. Part One. Quasi-continuous fragmentation. Sov. Astr. Lett. 10, 27–29.

Oberst, J., Molau, S., Heinlein, D., Grtizner, C., Schindler, M., Spurný, P., Ceplecha, Z., Rendtel, J., Betlem, H., 1998. The "European Fireball Network": Current status and future prospects. Meteorit. Planet. Sci. 33, 49–56.

Öpik, E.J., 1958. Physics of meteor flight in the atmosphere. Interscience, New York.

Pecina, P., Ceplecha, Z., 1983. New aspects in single-body meteor physics. Bull. Astron. Inst. Czech. 34, 102–121.

Pesnell, W.D., Grebowsky, J.M., 2000. Meteoric magnesium ions in the martian atmosphere. J. Geophys. Res. 105, 1695–1707.

Podolak, M.J., Pollack, J.B., Reynolds, R.T., 1988. Interactions of planetesimals with protoplanetary atmospheres. Icarus 73, 163–179.

Press, W.H., Teukolsky, S.A., Vetterling, W.T., Flannery, B.P., 1996. Numerical Recipes in F90, second ed. Cambridge Univ. Press, Cambridge, UK.

Prinn, R.G., Fegley Jr., B., 1987. The atmospheres of Venus, Earth and Mars: A critical comparsion. Annu. Rev. Earth Planet. Sci. 15, 171–212.

ReVelle, D.O., Ceplecha, Z., 2001. Bolide physical theory with application to PN and EN fireballs. In: Warmbein, B. (Ed.), Proc. Meteoroids 2001 Conf. ESA Publication Division, Noordwijk, The Netherlands, pp. 507–512.

Seiff, A., 1983. Appendix A: Models of Venus' atmospheric structure. In: Hunten, D.M., Colin, L., Donahue, T.M., Moroz, V.I. (Eds.), Venus. Univ. of Arizona Press, Tucson, pp. 1045–1048.

Shafrir, U., 1967. The effective braking height for small interplanetary particles in the martian upper atmosphere. Icarus 7, 100–104.

Shampine, L.F., Watts, H.A., 1977. The art of writing a Runge–Kutta code, Part I. In: Rice, J.R. (Ed.), Mathematical Software III. Academic Press, New York, pp. 257–275.

Vaubaillon, J., Colas, F., 2002. Evolution of a meteor stream and Leonids 2002 forecastings. In: Proc. Ast. Com. Met. 2002 Conf., pp. 181–184.

Whipple, F.L., 1938. Photographic meteor studies. Proc. Natl. Acad. Sci. 36, 687–695.

Whipple, F.L., 1950. The theory of micro-meteorites. Part I. In an isothermal atmosphere. Proc. Natl. Acad. Sci. 36, 687–695.

Whipple, F.L., 1951. The theory of micro-meteorites. Part II. In a heterothermal atmosphere. Proc. Natl. Acad. Sci. 37, 19–30.

Whipple, F.L., 1983. 1983 TB and the Geminid meteors. IAU Circ. 3881.

Williams, I.P., Wu, Z., 1993. The Geminid meteor stream and Asteroid 3200 Phaethon. Mon. Not. R. Astron. Soc. 262, 231–248.